

# Rapid Design of Mechanical Logic Based on Quasi-Static Electromechanical Modeling

Wenzhong Yan<sup>1,\*</sup>, Yunchen Yu<sup>1,\*</sup> and Ankur Mehta<sup>1</sup>

**Abstract**—Mechanical logic is a class of dynamic electromechanical mechanisms which leverages carefully designed mechanical structures to generate programmed control actions from a constant electrical power supply; thus, it can be employed as a control method for fully printable autonomous robots. Composed of a bistable buckled beam driven by conductive super-coiled polymer (CSCP) actuators, this type of electromechanical system features non-trivial relationships between its design parameters and resulting behavioral characteristics. In this paper we present an efficient method to rapidly design mechanical logic structures from desired behavioral specifications. We describe this dynamic system with a simplified, quasi-static model, whose validity is verified by time constant comparison. An analytical formula of the mechanical logic's behavioral characteristics, i.e. its oscillation period, is then derived as a simplified expression of the design parameters. Based on this expression, we formulate the design of mechanical logic from behavioral specifications into an optimization problem that maximizes the robustness to manufacturing tolerances, as demonstrated by an example case study.

## I. INTRODUCTION

Origami-inspired printable robots have been created to achieve inexpensive and rapid prototyping [1]; these robots are manufactured with cut-and-fold techniques, which allow designers to build complex 3D objects from 2D materials. Intensive efforts have been made to develop design tools [2], [3] and fabrication approaches [4], [5] for printable robots; however, their control methods are rarely investigated [6]. Recently, a new fully printable control strategy—mechanical logic—was invented [7]; we use one of its prototypes (Fig. 1) as our target of analysis in this paper. This mechanical logic incorporates a bistable mechanism that functions as a digital mechanical switch, along with CSCP actuators [8] that are composed of versatile conductive thread [9], [10] and function as the time delay relay. Under an electrical current, the actuators generate resistive heating to induce a temperature change, which transforms into mechanical energy through axial contraction. The actuators are connected to a bistable buckled beam, inducing its snap-through motions. Powered by a constant electrical energy source, this mechanism can autonomously sequence electrical actuation control signals. This mechanical logic is particularly noteworthy because it is inexpensive and easy-to-fabricate, highly apropos to printable robotics. While [7] is a preliminary investigation of mechanical logic, in this work we provide a mathematical description of this device to facilitate its design.

<sup>1</sup>Henry Samueli School of Engineering, University of California, Los Angeles, CA 90095. Please send correspondence to wzyan24@g.ucla.edu

\*These two authors contributed equally to this work.

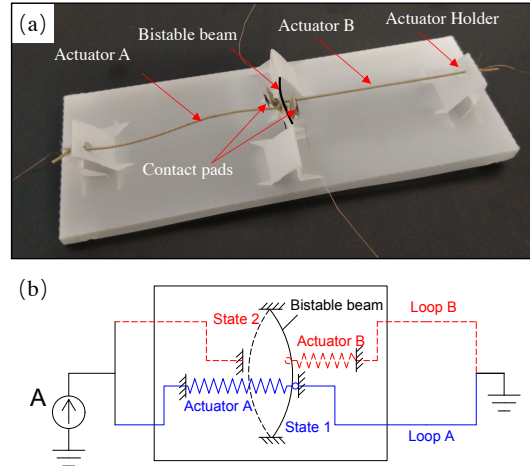


Fig. 1. Mechanical logic. (a) A prototype of the proposed mechanical logic ( $110 \times 40 \times 4 \text{ mm}$ ,  $1.75 \text{ g}$ ) [7]. (b) The mechanism of mechanical logic. Two loops are connected and disconnected alternatively when the bistable beam switches between the two different stable states, inducing current oscillation.

The basic configuration of this mechanical logic can be abstracted as a bistable mechanism driven by an actuator, which is found in many other processes and applications [11]–[15]; thus, this work's analysis can be extended to these other systems. The construction of such complex dynamic systems is usually bottlenecked by the design process, which involves numerous iterations of computationally expensive analysis. In order to efficiently customize and explore the functionality of this class of integrated mechanism in a rapid prototyping context, a systematic design method needs to be built. Bruch et al. [11] developed a model-based method to design pre-stressed buckled beams with specified snap-through characteristics. Gao et al. [16] also proposed a method for designing and fabricating bistable mechanisms with required snap-through behaviors. These studies utilized data-driven methods that required extensive computation. In this paper, we present an efficient formulation of mechanical logic design from behavioral specification as a low-complexity optimization problem.

Our design method is based on a quasi-static assumption that the mechanical logic's electrothermal subsystem (i.e. the actuators) features a much larger characteristic time constant compared to its mechanical subsystem (i.e. the bistable beam); thus, the behavior of the integrated system is dominated by the dynamics of the actuators. Under this assumption, we develop an analytical expression of the oscillation period of this mechanism based on our previous

work [17] on the analytical modeling of bistable buckled beams, which make up one subsystem of mechanical logic. With this analytical expression, we eventually transform the design of mechanical logic with a specified oscillation period into a set of constraints on the design parameters. To determine a specific parameter assignment, we can apply these constraints to an optimization criterion. In this work, we choose to maximize the robustness of the resulting design to manufacturing tolerances. As inevitable errors lead to inaccuracy in the realization of the design, we seek to minimize the resulting offset in the specified behavioral parameter after fabrication. This optimization-based method for the rapid design of mechanical logic is demonstrated with a case study. To summarize, our contributions include:

- a validated quasi-static modeling approach that characterizes a dynamic electromechanical system composed of a bistable beam driven by linear actuators;
- a computationally tractable analytical formula for the oscillation period, a behavioral characteristic of mechanical logic;
- an optimization formulation to rapidly design mechanical logic with desired high-level behavioral parameters while maximizing the robustness of design; and
- a case study that demonstrates this rapid design method.

The remainder of this paper is organized as follows: mechanical logic is introduced in Section II; the quasi-static model is derived and validated with FEA methods in Section III; the rapid design method and the formulated optimization problem are demonstrated with a case study in Section IV; and we end with some conclusions in Section V.

## II. BACKGROUND

Fig. 1 demonstrates one prototype of mechanical logic, which will be used as the target of our analysis.

### A. Description of the System

As shown in Fig. 1, this mechanical logic is composed of a bistable buckled beam and two CSCP actuators. One end of each actuator is attached to the bistable beam and the other end is fixed on the frame. The beam functions as a double-pole, single-throw switch for both Loop A and Loop B in opposite phases. The actuators serve two functions, one of which is to complete the circuitry, while the other is to drive the snap-through motion of the beam [7]. If the force generated by the actuator exceeds the activation force required by the bistable mechanism, a snap-through motion of the bistable mechanism is guaranteed. Under this circumstance, once power is supplied, this mechanical logic starts to oscillate, similar to an electrical oscillator.

### B. Model of Mechanical Logic

The symmetric structure and periodic motion of mechanical logic allow us to only consider its behavior within one single snap-through motion, as shown in Fig. 2. In this paper, the bistable mechanism is a clamped-clamped elastic buckled beam which is initially straight, and its behavior is described with a PDE [18]. The actuator is characterized with a thermo-electric-mechanical model [8].

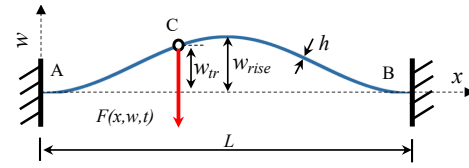


Fig. 2. A simplified model of mechanical logic. The actuation force  $F(x, w, t)$  from the actuator is applied at a specific point C with an initial displacement  $w_{\text{rise}}$ . The  $x$ -axis represents the line connecting the two ends (i.e. point A and B) of the beam, while the  $w$ -axis is set perpendicular to the  $x$ -axis at the left end (i.e. point A) of the beam.

1) *Bistable Beam*: The length, width, and thickness of the beam are denoted as  $L_0$ ,  $b$ , and  $h$ , respectively. The span of beam after buckling is denoted as  $L$ ; the difference between the original length and the span is denoted as  $d_0$ . The ratio  $\mu = (x_C - x_A)/(x_B - x_A)$  characterizes the position at which a point force  $F$  is applied. Assuming the Euler-Bernoulli beam model, the non-linear PDE that describes the displacement  $w(x, t)$  of the beam is as follows [18]:

$$EI \frac{\partial^4 w}{\partial x^4} + P \frac{\partial^2 w}{\partial x^2} - \frac{EA}{2L} \frac{\partial^2 w}{\partial x^2} \int_0^L \left( \frac{\partial w}{\partial x} \right)^2 dx + m \frac{\partial^2 w}{\partial t^2} + c \frac{\partial w}{\partial t} = F(x, w, t) \quad (1)$$

$$w(0, t) = \frac{\partial w}{\partial x}(0, t) = 0, \quad w(L, t) = \frac{\partial w}{\partial x}(L, t) = 0 \quad (2)$$

$$w(x, 0) = w_0(x) = \frac{w_{\text{rise}}}{2} \left[ 1 - \cos\left(\frac{2\pi x}{L}\right) \right]$$

where  $m$ ,  $E$ ,  $c$ ,  $P$ ,  $I$  ( $I = bh^3/12$ ) and  $A$  ( $A = bh$ ) refer to the mass per unit length, Young's modulus, viscous damping coefficient, axial loading, second moment, and cross-sectional area of the beam, respectively.  $w_0(x)$  refers to the initial displacement of the beam, while  $w_{\text{rise}}$  refers to the initial rise of the beam's midpoint.

2) *CSCP Actuator*: The thermo-electric-mechanical model of the actuator is as follows [8]:

$$F_a = k(x_a - x_0) + b_a \dot{x}_a + c_T(T - T_0) \quad (3)$$

where  $F_a$ ,  $x_a$  and  $x_0$  are the generated force, the loaded and unloaded length of the actuator, and  $k$ ,  $b_a$  are the mean stiffness and mean damping of the actuator, respectively.  $T$  is the temperature of the actuator,  $T_0$  is the room temperature (i.e. 25°C), and  $c_T$  is the mean slope that compensates the temperature rise. In order to simplify our model, we ignore the term  $b_a \dot{x}_a$ , as the effect of damping is considered negligible. The temperature rise of the actuator is described with Eq. 4, as derived from Yip's work [8]:

$$T(t) = \frac{U^2}{\lambda R} (1 - e^{-\frac{\lambda}{C_{th}} t}) + T_0 \quad (4)$$

where  $\lambda$  is the absolute thermal conductivity of the actuator in the ambient environment, while  $C_{th}$  and  $R$  refer to its thermal mass and resistance, respectively. The voltage  $U$  across the actuator is assumed constant in this work. The

relationships between some of the aforementioned parameters of the actuator and its length  $x_0$  are as follows:

$$k = \frac{\gamma_1}{x_0}, C_{th} = \gamma_2 x_0, \lambda = \gamma_3 x_0, R = \gamma_4 x_0 \quad (5)$$

where  $\gamma_1, \gamma_2, \gamma_3,$  and  $\gamma_4$  are associated with the environment, experimental setup, and properties of the actuator material.

### III. QUASI-STATIC APPROXIMATION FRAMEWORK

Here the dynamic model of mechanical logic is simplified under a quasi-static assumption. Ultimately an analytical formula of mechanical logic's oscillation period is derived.

#### A. Quasi-Static Assumption

To simplify our model, we make a quasi-static assumption that the electrothermal subsystem of mechanical logic features a significantly larger characteristic time constant than the mechanical subsystem. Thus, in response to the force generated by the actuator, the bistable beam is able to achieve equilibrium instantly. Therefore, the dynamics of the actuator dictates the behavior of the entire system. This quasi-static assumption is verified with FEA simulations. Moreover, we assume that the bistable beam settles instantly after snap-through motion, since it will immediately rest on a flexible contact pad with high damping [7].

#### B. Quasi-Static Assumption Verification

To validate our assumption, the time constants of both subsystems are evaluated and compared. The time constant of the mechanical subsystem (underdamped) is estimated as  $\tau_m = \pi / (w_n \sqrt{1 - \zeta^2})$  [19], where  $w_n$  and  $\zeta$  refer to the natural frequency and damping ratio of the system. In this work, we adopt the first-order natural frequency to calculate the time constant  $\tau_m$ . The time constant of the electrothermal subsystem, on the other hand, is given as  $\tau_{et} = C_{th} / \lambda$  [8]. To obtain the natural frequency  $w_n$  of the mechanical subsystem and explore the relationships between  $w_n$  and design parameters, several FEA models are built, with their design parameters listed in Table I. Specifically, Case 1 is used as the example to demonstrate the verification process.

1) *FEA Model*: The FEA model of the simplified mechanical subsystem is built with ABAQUS 2017, as shown in Fig.3(a). Both ends of the beam are fixed after precompression ( $d_0 = 0.6$  mm). One end of the actuator is connected to the beam at the location  $\mu = 0.43$  and the other end is fixed at a position that makes the actuator initially stress-free. The equivalent Young's modulus of the actuator is given by the equation  $E = kL/A$ . In the FEA model, the element Beam B21H is adopted for both the beam and the actuator.

2) *Time Constant Comparison*: The natural frequency corresponding to the first mode shape of the bistable beam in Case 1 is 706.3 Hz (Fig. 3(b)). Thus, with  $\zeta$  approximated as 0.5,  $\tau_m$  is calculated as  $5.7 \times 10^{-3}$  s. Meanwhile, with  $C_{ch}$  and  $\lambda$  measured as  $0.453$  Ws/ $^\circ$ C and  $0.249$  W/ $^\circ$ C, respectively,  $\tau_{et}$  can be calculated as 1.8 s. Since  $C_{ch}$  and  $\lambda$  both are proportional to the length of the actuator,  $\tau_{et}$  is constant. The natural frequency of the mechanical subsystem is highly insensitive to relevant design parameters. As shown in Case

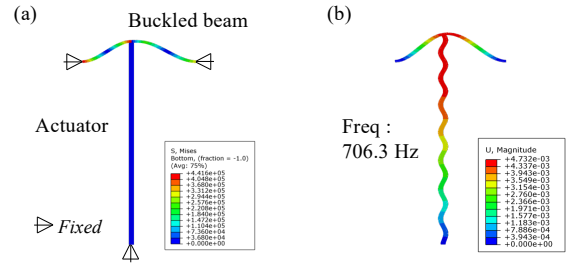


Fig. 3. FEA simulation (Case 1 in Table I). (a) FEA model. The beam is double-clamped and buckled under axial precompression. One end of the actuator is fixed and the other one is connected with the beam. (b) The first mode shape of the bistable beam with the corresponding natural frequency 706.30 Hz. The dimensions of the figure are adjusted for better presentation.

2-4 where we assign extreme values to different parameters, the resulting natural frequency is not significantly influenced by these changes (corresponding FEA simulation results are not shown since these cases have rather similar mode shapes to Case 1). Thus, within our range of consideration, the time constant of the electrothermal subsystem is always significantly larger than that of the mechanical subsystem.

TABLE I  
A TYPICAL SET OF PARAMETERS OF A MECHANICAL LOGIC.

Parameters	Unit	Case1	Case2	Case3	Case4
<i>Bistable beam :</i>					
Length ( $L_0$ )	mm	14.9	14.9	14.9	14.9
Width ( $b$ )	mm	3.0	1.0	3.0	3.0
Thickness ( $h$ )	mm	0.132	0.132	0.05	0.132
Precompression ( $d_0$ )	mm	0.6	0.6	0.6	0.05
Young's modulus ( $E$ )	GPa	3.0	3.0	3.0	3.0
Density ( $\rho$ )	g/cm <sup>3</sup>	1.38	1.38	1.38	1.38
Poisson's ratio ( $\nu$ )	1	0.50	0.50	0.50	0.50
<i>CSCP actuator :</i>					
Length ( $x_0$ )	mm	50.0	50.0	50.0	50.0
Diameter ( $D$ )	mm	0.8	0.8	0.8	0.8
Young's modulus ( $E$ )	MPa	18.6	18.6	18.6	18.6
Density ( $\rho$ )	g/cm <sup>3</sup>	1.15	1.15	1.15	1.15
Poisson's ratio ( $\nu$ )	1	0.50	0.50	0.50	0.50
Natural Freq.( $\omega$ )	Hz	706.3	706.3	574.6	706.3

#### C. A Reduced Model of Mechanical Logic

Under the quasi-static assumption, instead of solving Eq. 1 for  $w(x, t)$ , we perform time-stepping and solve for the beam's displacement at any time point in the actuation process, assuming that the beam reaches a static equilibrium. Thus, we can eliminate the time derivative terms in Eq. 1 and combine it with Eq. 3 with the damping term ignored. The resulting ODE describes the bistable beam's displacement at a specific time point  $t_i$ , as shown in Eq. 6 and Eq. 7.

$$EI \frac{d^4 w_i}{dx^4} + P \frac{d^2 w_i}{dx^2} - \frac{EA}{2L} \frac{d^2 w_i}{dx^2} \int_0^L \left( \frac{dw_i}{dx} \right)^2 dx = F \delta(x - \mu L) \quad (6)$$

$$F = -c_T[T(t_i) - T_0] - k[w_i(\mu L) - w_0(\mu L)] \quad (7)$$

In Eq. 6,  $w_i(x)$  denotes the displacement of the bistable beam at time  $t_i$  and satisfies the boundary conditions in Eq. 2. We transform the point force applied on the beam at the position  $x = \mu L$  into a distributive load with an equivalent actuation effect, utilizing the Dirac delta function. In Eq. 7,  $F$  is regarded as negative because it assumes the negative direction, as shown in Fig. 2. The magnitude of this point force at time  $t_i$  is also given by Eq. 7. This boundary value problem can be solved using the Galerkin method [20].

#### D. Analytical Expression of the Oscillation Period

As we assign different values to  $F$  in Eq. 6 and study the beam's corresponding equilibrium displacement at  $x = \mu L$ , we obtain a force-displacement curve of the bistable beam, as represented by the blue curve in Fig. 4. Also, Eq. 7 indicates a linear relationship between  $F$  and the difference between the loaded and unloaded length of the actuator at a given time point. Since the actuator is attached to the beam, this length difference is reflected by the beam's displacement at  $x = \mu L$ . Therefore, at any time point, there is a linear relationship between  $F$  and  $w(\mu L)$ , as demonstrated by the straight lines in Fig. 4. Thus the equilibrium displacement of

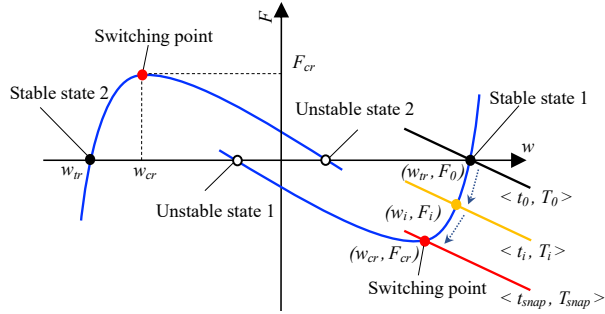


Fig. 4. The mechanism of the decoupled model of mechanical logic. Blue profiles are the force-displacement curves of the bistable buckled beam under off-center actuation; Straight lines are the force-displacement curves of the CSCP actuator at different temperature.

the bistable mechanism at  $x = \mu L$  at time  $t_i$  is characterized by the intersection of the invariant force-displacement curve of the bistable beam and the linear curve  $F - w_i(\mu L)$  that characterizes the force generated by the actuator at time  $t_i$ . At the beginning ( $t = t_0$ ), the linear curve is represented by the black line in Fig. 4 and intersects with the force-displacement curve at  $(w_{tr}, 0)$ , where  $w_{tr}$  refers to the initial displacement of the actuation position ( $w_0(\mu L) = w_{tr}$ ). As time elapses, the temperature of the actuator increases and the  $F - w_i(\mu L)$  curve moves downward, with the intersection of the two curves moving toward the switching point  $(w_{cr}, F_{cr})$ .

This representation of the equilibrium displacement of the bistable mechanism thus allows us to directly calculate the time needed for the bistable beam to reach the snap-through point, which, in this work, is assumed to be the switching point  $(w_{cr}, F_{cr})$ . In other words, we assume that the linear curve given by Eq. 7 at the snap-through time  $t_{snap}$  passes

through the switching point. Thus,  $t_{snap}$  satisfies the equation:

$$F_{cr} = -c_T[T(t_{snap}) - T_0] - k[w_{cr} - w_{tr}] \quad (8)$$

Combining Eq. 4 and Eq. 8, with the fact that the mechanical logic's oscillation period  $T_a$  is twice  $t_{snap}$ , we have:

$$T_a = -2 \frac{C_{th}}{\lambda} \ln \left[ 1 - \frac{\lambda R}{c_T U^2} (k w_{tr} - k w_{cr} - F_{cr}) \right] \quad (9)$$

The beam's snap-through characteristics,  $w_{tr}$ ,  $w_{cr}$ , and  $F_{cr}$ , are extracted from its force-displacement curve. Studying Eq. 6 by changing the magnitude of  $F$  and calculating the corresponding displacement of the beam is one possible way to obtain the force-displacement curve, and curves generated with other methods (e.g. experiments) also apply, as long as the parameters  $w_{tr}$ ,  $w_{cr}$ , and  $F_{cr}$  can be evaluated from these curves. In this paper, we utilize the results from our previous work, where we derived analytical formulas of  $w_{tr}$ ,  $w_{cr}$ , and  $F_{cr}$  as expressions of the design parameters of the beam [17]:

$$\begin{aligned} w_{tr} &= \frac{\sqrt{d_0 L}}{\pi} [1 - \cos(2\pi\mu)] \\ w_{cr} &= 2\sqrt{d_0 L} \bar{w}(\mu), \quad F_{cr} = -\frac{EI\sqrt{d_0 L}}{L^3} \bar{F}(\mu) \\ \bar{w}(\mu) &= -7.155\mu^4 + 2.872\mu^3 + 4.339\mu^2 - 1.538\mu + 0.0832 \\ \bar{F}(\mu) &= 50588\mu^4 - 69285\mu^3 + 36606\mu^2 - 8894.5\mu + 914.9 \end{aligned} \quad (10)$$

with  $\mu \in [0.35, 0.5]$

Eq. 9 and Eq. 10 combined yield an analytical formula of the mechanical logic's oscillation period as an expression of its design parameters. It is worth noting that determining the snap-through point of bistable beams connected to actuators is a challenge by itself. In this paper, we assume that the snap-through point coincides with the switching point of the beam for convenience; there might be other possible locations of the snap-through point, which we may investigate in the future to improve our model.

## IV. DESIGN METHOD AND EVALUATION

Our analytical model of the mechanical logic's oscillation period effectively guides the design of the system when a desired oscillation period is specified. Here we demonstrate one possible optimization algorithm that finds the set of design parameters that allows the mechanical logic to oscillate at a desired period and at the same time, maximizes the robustness of design and thus improves the manufacturability of the resulting system. Importantly, users can customize their own, specific constrained optimization problems, with different degrees of freedom or parameters to be optimized, using the scheme to be discussed. The functionality of this algorithm is further demonstrated with a case study.

### A. Optimization Problem Formulation

1) *Parameters and Constraints:* We consider a mechanical logic with the following predetermined parameters: the temperature change compensation term  $c_T$ , the voltage across the actuator  $U$ , as well as the parameters  $\gamma_1, \gamma_2, \gamma_3, \gamma_4$  that characterize the relationships between  $k, C_{th}, \lambda$ , and

$R$  and the length of the actuator  $x_0$ , as given in Eq. 5. Moreover, we assume that some design parameters, namely the thickness of the beam  $h$ , the Young's modulus  $E$ , and the actuation position  $\mu$ , are predetermined by users. All of these aforementioned parameters are summarized in Table II.

The remaining design parameters to be optimized include the width of the beam  $b$ , the original length  $L_0$ , the span  $L$ , and the length of the actuator  $x_0$ , all of which are subject to certain constraints. Constraints on  $b$ ,  $L_0$ , and  $x_0$  are specified by users, as shown in Table II. Moreover, the analytical models of the snap-through characteristics in Eq. 10 are highly accurate if the precompression rate is less than 8% [17], indicating an implicit constraint on  $L$  and  $L_0$ .

More constraints may be imposed on the parameters if the system has limitations for the critical snap-through force or critical displacement. For instance, if the system is unable to provide actuation force that exceeds a certain magnitude, another constraint on the design parameters may be relevant.

2) *Optimization*: As different designs of the mechanical logic may yield the same oscillation period, we choose the design with the highest robustness. Given the inevitable fabrication errors that would result in some inaccuracy in the values of design parameters, we want to minimize the ultimate error in the oscillation period  $T_{osc}$ . Fabrication tools such as laser cutters typically result in inaccuracy in the geometry of the beam, while manually cutting the actuator may result in inaccuracy in its length. Thus, the robustness of a set of design parameters is associated with the partial derivatives  $\partial T_a / \partial b$ ,  $\partial T_a / \partial L_0$ ,  $\partial T_a / \partial L$ , and  $\partial T_a / \partial x_0$  when this set of parameters is adopted. Hence, our optimization problem minimizes the absolute values of these partial derivatives:

$$\begin{aligned}
& \underset{b, L_0, L, x_0}{\text{minimize}} && \mathbf{g}^T \mathcal{E} \mathbf{g} \\
& \text{subject to} && T_a(b, L_0, L, x_0) = T_{osc} \\
& && b^{min} \leq b \leq b^{max} \\
& && L_0^{min} \leq L_0 \leq L_0^{max} \\
& && 0 \leq \frac{L_0 - L}{L_0} \leq 0.08 \\
& && x_0^{min} \leq x_0 \leq x_0^{max}. \\
& \text{with} && \mathbf{g} = \nabla T_a = \left\langle \frac{\partial T_a}{\partial b}, \frac{\partial T_a}{\partial L_0}, \frac{\partial T_a}{\partial L}, \frac{\partial T_a}{\partial x_0} \right\rangle^T \\
& && \mathcal{E} = \text{diag}(e_b^2, e_{L_0}^2, e_L^2, e_{x_0}^2)
\end{aligned} \tag{11}$$

Note that we write  $T_a$  as a function of  $b$ ,  $L_0$ ,  $L$ , and  $x_0$  for simplicity, but  $T_a$  also depends on the predetermined parameters in Table II.  $\mathcal{E}$  contains the weight of each partial derivatives in the cost function  $\mathbf{g}^T \mathcal{E} \mathbf{g}$ . The weights are given as the estimated fabrication error bounds for  $b$ ,  $L_0$ ,  $L$ , and  $x_0$ , which are dependent on the fabrication methods and therefore inputted by users. This optimization problem, with constraints and the weight matrix  $\mathcal{E}$  customized by users, can be solved with `fmincon` in MATLAB.

### B. Case Study

We consider a mechanical logic whose predetermined parameters are given in Table II. The bistable beam is made of

polyester (PET) sheet, whose thickness and elastic modulus are 0.132 mm and 3 GPa, respectively. The actuation position parameter  $\mu$  is chosen as 0.43 and the constraints on the geometry of the beam and the actuator are given in Table II. The oscillation period is chosen as 4.0 s. Since the bistable

TABLE II  
PARAMETERS AND CONSTANTS IN THE OPTIMIZATION PROBLEM.

Parameter	Unit	Case Study
<i>Predetermined Parameters :</i>		
Mean Stiffness Const ( $\gamma_1$ )	$N$	9.34
Thermal Mass Const ( $\gamma_2$ )	$N/^\circ C$	9.06
Thermal Conductivity Const ( $\gamma_3$ )	$N/(s \cdot ^\circ C)$	4.98
Resistance Const ( $\gamma_4$ )	$\Omega/m$	277.67
Voltage ( $U$ )	$V$	7.64
Temperature Compensation ( $c_T$ )	$N/^\circ C$	0.0286
Beam Thickness ( $h$ )	mm	0.132
Beam Young's modulus ( $E$ )	GPa	3.0
Actuation Position ( $\mu$ )	1	0.43
<i>Constraints :</i>		
Min Beam Width ( $b^{min}$ )	mm	2.5
Max Beam Width ( $b^{max}$ )	mm	3.5
Min Beam Length ( $L_0^{min}$ )	mm	12.0
Max Beam Length ( $L_0^{max}$ )	mm	24.0
Min Actuator Length ( $x_0^{min}$ )	mm	40.0
Max Actuator Length ( $x_0^{max}$ )	mm	100.0

beam is folded from a 2D pattern fabricated with a laser cutter [7], the laser kerf, approximately 0.1 mm wide [21], may result in inaccuracy in  $b$ ,  $L$ , and  $L_0$ . We choose the error bounds of  $b$ ,  $L_0$ , and  $L$  as twice of the width of the laser kerf. Meanwhile, we choose the error bound of  $x_0$  as 0.6 mm, as cutting the CSCP actuator manually might involve larger error. Therefore, the entries in the weight matrix  $\mathcal{E}$ ,  $e_b$ ,  $e_{L_0}$ ,  $e_L$ , and  $e_{x_0}$ , are chosen as  $0.2 \times 10^{-3}$ ,  $0.2 \times 10^{-3}$ ,  $0.2 \times 10^{-3}$ , and  $0.6 \times 10^{-3}$ .

The values of  $b$ ,  $L_0$ ,  $L$ , and  $x_0$  given by the optimization are 2.5 mm, 24.0 mm, 22.1 mm, and 52.8 mm, respectively. The robustness of this design is tested and compared with the robustness of another design that yields the same oscillation period ( $b = 3.0$  mm,  $L_0 = 15.0$  mm,  $L = 14.5$  mm,  $x_0 = 64.0$  mm). In Table III, Case 1 and Case 6 represent ideal circumstances where no fabrication error occurs, while Case 2-5 and Case 7-10 represent those where there are significant errors in  $b$ ,  $L_0$ ,  $L$ , and  $x_0$ . There is an one-to-one correspondence between these cases, as the errors in these four parameters are exactly the same in Case 2 and Case 7 and this pattern holds in the other three pairs of test cases.

The small relative error in the oscillation period from Case 2-5 indicates that the parameters suggested by the algorithm feature high robustness in design. Even when fabrication errors are highly notable, we can still keep the error in the oscillation period within  $\pm 10\%$ . In Case 7-10 (compared to Case 6), the absolute errors in  $b$ ,  $L_0$ ,  $L$ , and  $x_0$  are also 0.1 mm, 0.1 mm, 0.1 mm, and 0.3 mm, respectively, but these errors make the relative error in the oscillation period exceed 30% in multiple cases. Also, each of Case 7-10 has notably

larger relative error than their corresponding case from 2-5. These observations indicate that our arbitrary choice of design parameters has much lower robustness.

Importantly, these robust design parameters are obtained nearly instantly by running the optimization algorithm on a typical personal computer, while conventional parameter exploration would have been extremely time-consuming.

TABLE III

EXAMPLE TEST CASES THAT DEMONSTRATE DESIGN ROBUSTNESS.

Case	$b$ mm	$L_0$ mm	$L$ mm	$x_0$ mm	$T_{osc}$ s	Error %	
1*	2.5	24.0	22.1	52.8	4.00	0	
2	2.4	24.1	22.2	53.1	3.97	-0.75	
Optimized	3	2.4	24.1	22.0	52.5	4.26	+6.50
4	2.6	23.9	22.0	53.1	4.13	+3.25	
5	2.6	23.9	22.2	52.5	3.64	-9.00	
6*	3.0	15.0	14.5	64.0	4.00	0	
7	2.9	15.1	14.6	64.3	3.83	-4.25	
Naive	8	2.9	15.1	14.4	63.7	5.40	+35.0
9	3.1	14.9	14.4	64.3	4.28	+7.00	
10	3.1	14.9	14.6	63.7	2.65	-33.8	

Note: \* represents ideal cases while the others refer to cases where there are significant errors in  $b$ ,  $L_0$ ,  $L$ , and  $x_0$ .

## V. CONCLUSION

We have proposed a rapid design method for mechanical logic, a complex dynamic electromechanical system composed of a bistable buckled beam and CSCP actuators. Based on a quasi-static model, we have developed an analytical expression for our mechanical logic's oscillation period. With this analytical expression, the design of mechanical logic from desired behavioral specifications is formulated into a constrained optimization problem, which takes as input predetermined parameters of the system and, after performing optimization instantly, outputs a set of design parameters that allows the mechanical logic to oscillate at the desired period and maximizes the robustness of the design.

Beyond the scope of the mechanical logic discussed in this work, our design method may apply to other dynamic electromechanical systems satisfying the quasi-static assumption. For instance, we can replace the CSCP actuator with shape memory alloy (SMA) actuator [22] or replace the bistable beam with a monostable beam [23]. Given the high simplicity and flexibility of our method, we believe that our work can facilitate the modeling, designing, and prototyping of many complicated dynamic compound systems with similar basic configurations to that of mechanical logic.

## ACKNOWLEDGMENTS

This work is partially supported by the National Science Foundation under grants #1644579 and #1752575. The authors are grateful to Prof. Lihua Jin and Mr. Yuzhen Chen for the discussion on the FEA modeling.

## REFERENCES

- [1] C. D. Onal, R. J. Wood, and D. Rus, "An origami-inspired approach to worm robots," *IEEE/ASME Transactions on Mechatronics*, vol. 18, no. 2, pp. 430–438, 2013.
- [2] A. M. Mehta, J. DelPreto, B. Shaya, and D. Rus, "Cogeneration of mechanical, electrical, and software designs for printable robots from structural specifications," in *2014 IEEE/RSJ International Conference on Intelligent Robots and Systems*, 2014, pp. 2892–2897.
- [3] A. M. Mehta, J. DelPreto, K. W. Wong, S. Hamill, H. Kress-Gazit, and D. Rus, *Robot Creation from Functional Specifications*, 2018, pp. 631–648.
- [4] C. D. Onal, M. T. Tolley, R. J. Wood, and D. Rus, "Origami-inspired printed robots," *IEEE/ASME Transactions on Mechatronics*, vol. 20, no. 5, pp. 2214–2221, 2015.
- [5] E. A. Peraza-Hernandez, D. J. Hartl, R. J. M. Jr, and D. C. Lagoudas, "Origami-inspired active structures: a synthesis and review," *Smart Materials and Structures*, vol. 23, no. 9, p. 094001, 2014.
- [6] D. Rus and M. T. Tolley, "Design, fabrication and control of origami robots," *Nature Reviews Materials*, vol. 3, no. 6, pp. 101–112, 2018.
- [7] W. Yan, A. Gao, Y. Yu, and A. Mehta, "Towards autonomous printable robotics: Design and prototyping of the mechanical logic," *International Symposium on Experimental Robotics*, 2019 (In Press).
- [8] M. C. Yip and G. Niemeyer, "On the control and properties of supercoiled polymer artificial muscles," *IEEE Transactions on Robotics*, vol. 33, no. 3, pp. 689–699, June 2017.
- [9] D. Zhang and Y. Rahmat-Samii, "A novel flexible electro-textile 3t mri rf coil array for carotid artery imaging: Design, characterization and prototyping," *IEEE Transactions on Antennas and Propagation*, pp. 1–1, 2019.
- [10] D. Zhang and Y. Rahmat-Samii, "Integration of electro-textile rf coil array with magnetic resonance imaging (mri) system: Design strategies and characterization methods," in *2018 International Workshop on Antenna Technology (iWAT)*, March 2018, pp. 1–3.
- [11] D. Bruch, S. Hau, P. Loew, G. Rizzello, and S. Seelecke, "Fast model-based dielectric elastomer membrane actuators biased with pre-stressed buckled beams," pp. 10 594 – 10 594 – 8, 2018.
- [12] A. Crivaro, R. Sheridan, M. Frecker, T. W. Simpson, and P. Von Lockette, "Bistable compliant mechanism using magneto active elastomer actuation," *Journal of Intelligent Material Systems and Structures*, vol. 27, no. 15, pp. 2049–2061, Aug. 2016.
- [13] J.-H. Han, R. Addo-Akoto, J.-S. Han, J.-E. Suh, and J. Lee, "Buckled bistable beam actuation with twisted strings," in *Active and Passive Smart Structures and Integrated Systems XII*, A. Erturk, Ed. Denver, United States: SPIE, Mar. 2018, p. 30.
- [14] T. Li, Z. Zou, G. Mao, and S. Qu, "Electromechanical bistable behavior of a novel dielectric elastomer actuator," *Journal of Applied Mechanics*, vol. 81, no. 4, p. 041019, Nov. 2013.
- [15] L. Medina, R. Gilat, B. Ilic, and S. Krylov, "Two-directional operation of bistable latchable micro switch actuated by a single electrode," *Proceedings*, vol. 1, no. 4, p. 277, Aug. 2017.
- [16] R. Gao, M. Li, Q. Wang, J. Zhao, and S. Liu, "A novel design method of bistable structures with required snap-through properties," *Sensors and Actuators A: Physical*, vol. 272, pp. 295 – 300, 2018.
- [17] W. Yan, Y. Yu, and A. Mehta, "Analytical modeling for rapid design of bistable buckled beams," *Theoretical and Applied Mechanics Letters*, 2019 (In Press).
- [18] A. Nayfeh and R. Ibrahim, "Nonlinear interactions: analytical, computational, and experimental methods," *Applied Mechanics Reviews*, vol. 54, p. B60, 2001.
- [19] S. S. Rao and F. F. Yap, *Mechanical vibrations*. Prentice hall Upper Saddle River, 2011, vol. 4.
- [20] H. M. Ouakad and M. I. Younis, "The dynamic behavior of MEMS arch resonators actuated electrically," *International Journal of Non-Linear Mechanics*, vol. 45, no. 7, pp. 704–713, Sept. 2010.
- [21] C.-T. Pan, H. Yang, M.-K. Wei, and F.-Y. Chang, "Pet polymer ablation using excimer laser for nozzle plate application," *Materials Science and Technology*, vol. 23, no. 8, pp. 980–986, Aug. 2007.
- [22] J. Hong, W. Yan, Y. Ma, D. Zhang, and X. Yang, "Experimental investigation on the vibration tuning of a shell with a shape memory alloy ring," *Smart Materials and Structures*, vol. 24, no. 10, p. 105007, Sept. 2015.
- [23] J. Qiu, J. Lang, and A. Slocum, "A curved-beam bistable mechanism," *Journal of Microelectromechanical Systems*, vol. 13, no. 2, pp. 137–146, Apr. 2004.